Materials Research Express

PAPER

Bio-green synthesis of Ag–GO, Au–GO and Ag–Au–GO nanocomposites using *Azadirachta indica*: its application in SERS and cell viability

RECEIVED
11 December 2015

REVISED
1 June 2016

ACCEPTED FOR PUBLICATION
14 June 2016

PUBLISHED
21 July 2016

K Hareesh[1], J F Williams[2], N A Dhole[3], K M Kodam[3], V N Bhoraskar[1] and S D Dhole[1]

[1] Department of Physics, Savitribai Phule Pune University, Pune-411007, India
[2] School of Physics, University of Western Australia, Crawley, WA-6009, Australia
[3] Department of Chemistry, Savitribai Phule Pune University, Pune-411007, India

E-mail: appi.2907@gmail.com **and** sanjay@physics.unipune.ac.in

Keywords: graphene oxide, nanocomposites, Neem leaves extract, SERS, cell viability

Supplementary material for this article is available online

Abstract

Silver-graphene oxide, Gold–graphene oxide, Silver–Gold–graphene oxide nanocomposites were synthesized from Neem leaves (*Azadirachta indica*) extract using a bio-green one-pot method. The synthesized bio-green nanocomposites were characterized by UV–visible spectroscopy, x-ray diffractogram, transmission electron microscopy, x-ray photoelectron spectroscopy and Raman spectroscopy. The results indicated the decoration of ~10 nm of silver, ~20 nm of gold and ~15 nm of silver–gold nanoparticles on a graphene oxide sheet. The synthesized nanocomposites showed enhancement in surface enhanced Raman spectroscopy with alizarin and also enhancement in cell viability of Chang liver cell lines which may be due to a synergetic effect of nanoparticles and graphene oxide.

1. Introduction

Graphene oxide (GO) is considered as an analog of graphene which is obtained by the chemical treatment of graphite through oxidation, with subsequent dispersion in water or suitable organic solvents [1]. GO exhibits large amount of oxygen functional groups such as hydroxyl, carbonyl, carboxyl and epoxy groups on its basal plane and edges [2]. These functional groups allow nanoparticles to interact with the GO sheets through physisorption, electrostatic binding or charge-transfer interactions [3]. In particular, carboxylic moieties on a GO surface can stabilize the active metal ion species that can attach directly to the carboxyl groups. Thus, the reduction takes place on the surface of the GO sheets, giving one-step formation of nanoparticles attached to the GO sheets without the need for functionalization [4].

Different kinds of nanoparticles such as silver (Ag) [5], gold (Au) [6], copper [7], CeO_2 [8], Ag–Au [9] can decorate GO with more attention given to Ag and Au nanoparticles on GO because of their application in various fields such as sensors [10, 11] photocatalytic [12, 13], solar cell [14], electrochemical capacitor [15], SERS [16, 17], antimicrobial [18], drug-resistant cancer treatment [19], magnetic hyperthermia therapy [20] etc. These classes of nanocomposites can be synthesized by different methods, viz. hydrothermal [21, 22], rudimentary [10], chemical reduction [23, 24], ultrasonication [25, 26], UV-radiation [27], gamma radiation [28], electron beam assisted method [29] and a green methods [30–32].

A green method is a simple, low-cost, environmental friendly method which uses products and processes that minimize the use and generation of hazardous substances and does not require high temperature or harsh reducing agent [33]. Also, the nanocomposites synthesized by this method showed enhanced biological applications such as anti-microbial properties [24, 31, 32], enhanced cell viability [34, 35] etc which make them attractive in biological applications.

Neem, known as *Azadirachta indica*, contains phytochemicals like alkaloids, flavonoids, terpenoids, carotenoids, steroids and biologically active compounds such as salannin, volatile oils, meliantriol and nimbin (a triterpenoid). Neem leaf is very effective in treating some diseases like ringworm, acne, gangrene at developing conditions, and to heal chronic wounds [36]. It is also used as anti-inflammatory, anti-hyperglycaemic, anticancer agent etc [36]. It is believed to remove toxins from the body and neutralize free radicals [36]. The phytochemicals viz. flavonoids and terpenoids which are in Neem leaf extract adsorb on the metal nanoparticles surface and acts as capping species. The presence of reducing sugar in Neem leaf extract could be responsible for the reduction of metal ions and formation of corresponding metal nanoparticles [37]. There are many reports for the synthesis of Ag and Au nanoparticles using Neem extract. Shankar *et al* [37] have synthesized Au, Ag and Au–Ag nanoparticles using *Azadirachta indica* leaf broth. Green synthesis of Au nanoparticles (AuNPs) using *Azadirachta indica* leaves extract has been reported by Bindhani and Panigrahi [38]. Ahmed *et al* [39] have used aqueous leaf extract of *Azadirachta indica* for the synthesis of Ag nanoparticles (AgNPs). The antimicrobial property and toxicity analysis of *Azadirachta indica* synthesized AgNPs has been studied by Banerjee *et al* [40]. Prathna *et al* [41] have reported the kinetic evolution of studies of AgNPs synthesized using *Azadirachta indica*. The AgNPs of different shape have been synthesized using *Azadirachta indica* in the presence of cetyltrimethylammonium bromide by Khan *et al* [42]. However, there is a lacuna in literature survey regarding the synthesis of Ag–GO, Au–GO and Ag–Au–GO nanocomposite using *Azadirachta indica* and their application in SERS and cell viability.

Therefore, herein, we report the green synthesis of Ag–GO, Au–GO and Ag–Au–GO nanocomposites using *Azadirachta indica* leaves extract through a green one-pot method. The synthesized nanocomposites have been characterized by UV–visible spectroscopy, x-ray diffractogram (XRD), transmission electron microscopy (TEM), Raman spectroscopy and x-ray photoelectron spectroscopy (XPS). The SERS application with alizarin and the cell viability using Chang liver cell lines has been studied for synthesized nanocomposites.

2. Experimental

Graphite powder, sodium nitrate, (99%), sulfuric acid, hydrogen peroxide, potassium permanganate (99%), silver nitrate ($AgNO_3$) (99%), chloroauric acid ($HAuCl_4$) and alizarin were purchased from Sigma-Aldrich (USA). Fresh Neem leaves were collected from the local Indian market. All other chemicals used in the present work were of analytical grade unless otherwise specified. All the glasswares were thoroughly washed by double distilled water before use. Chang liver cell lines were collected from National Centre for Cell Science, Pune, India.

2.1. Preparation of Neem leaves extract

The fresh Neem leaves were washed twice with double distilled water. Then, 10 g of Neem leaves were crushed and boiled in 100 ml of double distilled water at 80 °C for 30 min. Then, it was centrifuged and supernatant was filtered through a 0.22 μm membrane to further remove of any trace solid residues.

2.2. Synthesis of GO, Ag–GO, Au–GO and Ag–Au–GO nanocomposites

GO was synthesized by modified Hummers' method [43]. In brief, graphite powder (0.5 g), sodium nitrate (0.5 g) and sulfuric acid (23 ml) were mixed in an ice-bath with continuous stirring. Potassium permanganate (3.0 g) was slowly added into the reaction mixture at 20 °C in a flask which was then transferred to water bath (35 $\perp$ 5) °C and the solution stirred for an hour to form a thick paste. 100 ml water was added and temperature of the bath was raised to (90 $\perp$ 5) °C under constant stirring for another 15 min. The solution was diluted by adding 500 ml water and subsequently 3 ml hydrogen peroxide (30% v/v) was added which led to a color change from dark brown to yellow. The mixture was filtered and washed several times with hot water to eliminate the acid residue. The resultant solid was dried under vacuum and stored in a desiccator. This prepared GO was dispersed in double distilled water (0.25 mg ml^{-1}) and sonicated for 1 h. Then, 5 ml of 10 mM $AgNO_3$, 5 ml of 10 mM $HAuCl_4$ and 3 ml of Neem leaves extract was added to 20 ml of GO, and kept at 25 °C in an autoclave. After 24 h, the sample was removed from an autoclave, centrifuged, washed with double distilled water several times to remove unreacted Neem extract and redispersed in water for characterization. The resulting nanocomposite is called Ag–Au–GO. With other conditions being the same, 10 ml of $AgNO_3$ was used for Ag–GO and 10 ml of $HAuCl_4$ was used for Au–GO nanocomposites.

2.3. Characterization of the nanocomposites

UV–visible spectroscopy for all the samples was carried out using a JASCO, V-670 UV–visible spectrophotometer. XRD analysis was done using a Bruker AXS D8 Advance x-ray diffractometer with a CuK_α source. The surface morphology was studied using TEM with model Tecnai G^2 U-thin 200 kV, LaB_6 filament.

Raman spectroscopic measurements were carried out using a Renishaw Invia laser Raman microscope with laser excitation wavelength of 634 nm. XPS was performed in an ultrahigh vacuum chamber with a base pressure below 8×10^{-7} Pa at room temperature.

To study the SERS of synthesized nanocomposites with alizarin, 100 μl of nanocomposite (1 mg ml^{-1}) was drop casted on to glass substrate and dried. Then, 100 μl of 2×10^{-4} M alizarin was drop casted on top of the nanocomposites and allowed to dry at room temperature. Then, the SERS was measured for all the samples at 634 nm.

2.4. Determination of cell viability

An MTT colorimetric assay was made to access cell viability with slight modification of reported method [41]. The Chang liver cells were harvested (10×10^4 cells/well) and inoculated in 96 well microtiter plates. The cells were washed with phosphate buffered saline (PBS) and the cultured cells were inoculated, with and without, test samples at different concentration of 10, 25, 50, 75 and 100 μg ml^{-1} and incubated for 24 h in CO_2 incubator (Nuaire, USA). After 24 h incubation, the medium was aspirated. 20 μl of 3-(4,5-dimethylthiazol-2-yl)-2,5-diphenyltetrazolium bromide (MTT) solution (5 mg ml^{-1} in PBS, pH 7.2) is added to each well and the plates are incubated for 4 h at 37 °C. The MTT was decanted and the formazan crystals formed were dissolved by addition of 80 μl of Dimethyl sulphoxide to the wells followed by gentle shaking for 10 min. The absorbance was read at 540 nm in a multiplate reader (PerkinElmer, USA) and surviving cell fraction was calculated. Hydrogen peroxide (100 μg ml^{-1}) was used as reference. The percent of cell viability was calculated by the formula: percent viability = (1- absorbance of treated cells/absorbance of untreated cells) x100.

3. Results and discussion

3.1. Characterization of the nanocomposites

Figure 1 shows the UV–visible absorbance spectra of Ag–GO, Au–GO and Ag–Au–GO nanocomposite, and that of GO is shown in figure S1 (ESI). GO showed two peaks around 230 and 296 nm respectively corresponding to π–π^* transition of aromatic C–C bond and n–π^* transition of C=C bond as can be seen from figure S1 [43]. UV–visible spectrum for Ag–GO, Au–GO, Ag–Au–GO nanocomposite was recorded after 4h , 8h , 16h , 24 h of mixing $AgNO_3$, $HAuCl_4$ and Neem leaves extract into GO. After 4 h, a peak centered on 433 nm appears in case of Ag–GO nanocomposite as shown in figure 1(a). This corresponds to surface plasmon resonance of AgNPs [10]. The absorbance of this peak increased with increase in time indicating the formation of more AgNPs up to 24 h. After 24 h, the absorbance was almost the same. Similarly, for the Au–GO nanocomposite, a peak centered on 566 nm appeared corresponding to a surface plasmon resonance of AuNPs as shown in figure 1(b) [27]. In this case also, the absorbance of AuNPs increased with increase in time revealing the formation of more AuNPs. After 24 h, the absorbance was the same. As can be seen from figure 1(c), Ag–Au–GO nanocomposite showed a broad peak centered on 480 nm and that result confirms the formation of Ag–Au mixed alloy nanoparticles. Wu *et al* [9] have reported that the mixed alloy nanoparticles have only one absorbance peak whose position is between the peaks of pure nanoparticles. For this increase in time indicating the more formation of Ag–Au nanoparticles and more absorbance was found at 24 h.

The formation of Ag, Au and Ag–Au nanoparticles can be explained as follows. The Neem leaf extract contains many biomolecules like flavonoids, terpenoids, alkaloids, alcoholic compounds, ascorbic acid, polysaccharides, saponins, β-phenylethylamines, reducing sugar and proteins/enzymes [36]. However, some glucose and ascorbate reduce $AgNO_3$ and $HAuCl_4$ to Ag^+ and Au_3^-. The terpenoids, flavonoids and reducing sugars present in leaf extract will reduce these Ag^+ and Au_3^- to their respective nanoparticles [37]. These formed Ag, Au and Ag–Au nanoparticles will get interact with GO through oxygen functional groups and decorated on GO.

The results of XRD, used to study the crystallographic structure of prepared Ag–GO, Au–GO and Ag–Au–GO nanocomposites is shown in figure 2 and for GO is in figure S2 (ESI). GO exhibited its characteristic peak around 10.63° corresponding to (001) plane. All the nanocomposites exhibit peaks at 38.06°, 44.59°, 64.63° and 77.54° respectively corresponding to the planes (111), (200), (220) and (311) planes confirming the formation of face centered cubic structure Ag, Au and Ag–Au nanoparticles [37]. The d-spacing for the plane (111) is found to be 2.36 Å which is also supported by TEM results, explained in later section. The peak for GO was masked due to the strong reflection from silver and gold nanoparticles.

TEM images of Ag–GO, Au–GO and Ag–Au–GO nanocomposites are shown in figure 3. Figures 3(a), (c) and (e) shows the decoration of Ag, Au and Ag–Au NPs of size ~10 nm, ~20 nm and ~15 nm respectively on GO. The d-spacing of nanocomposites is found to be ~2.36 Å representing (111) plane formation as can be seen from figures 3(b), (d) and (f) which is in agreement with XRD results. The corresponding inset figures show that the nanoparticles Ag, Au and Ag–Au have good crystalline structure in their respective nanocomposites.

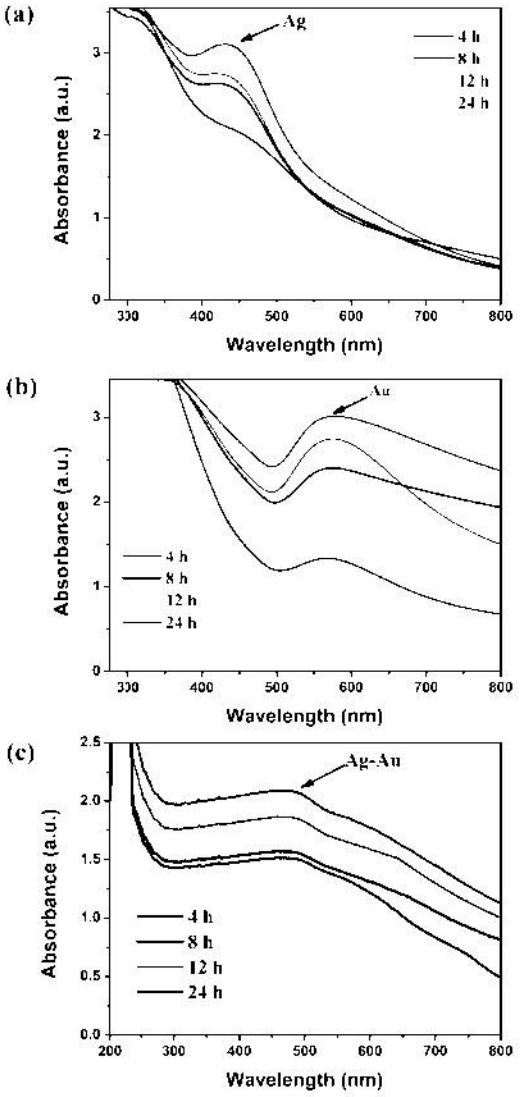

Figure 1. UV–visible spectroscopy of (a) Ag–GO, (b) Au–GO and (c) Ag–Au–GO nanocomposites.

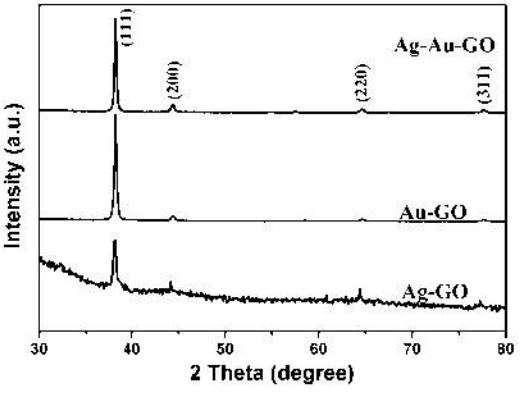

Figure 2. XRD of Ag–GO, Au–GO and Ag–Au–GO nanocomposites.

Further, we used XPS to study the structural properties of Ag–GO, Au–GO and Ag–Au–GO nanocomposites. Figure 1(a) shows the XPS survey spectra for GO, Ag–GO, Au–GO and Ag–Au–GO nanocomposites. These data confirm the presence of Ag, Au and Ag–Au respectively in Ag–GO, Au–GO and Ag–Au–GO nanocomposites. Figure 1(b) shows the high resolution C1s XPS spectra of GO indicating the

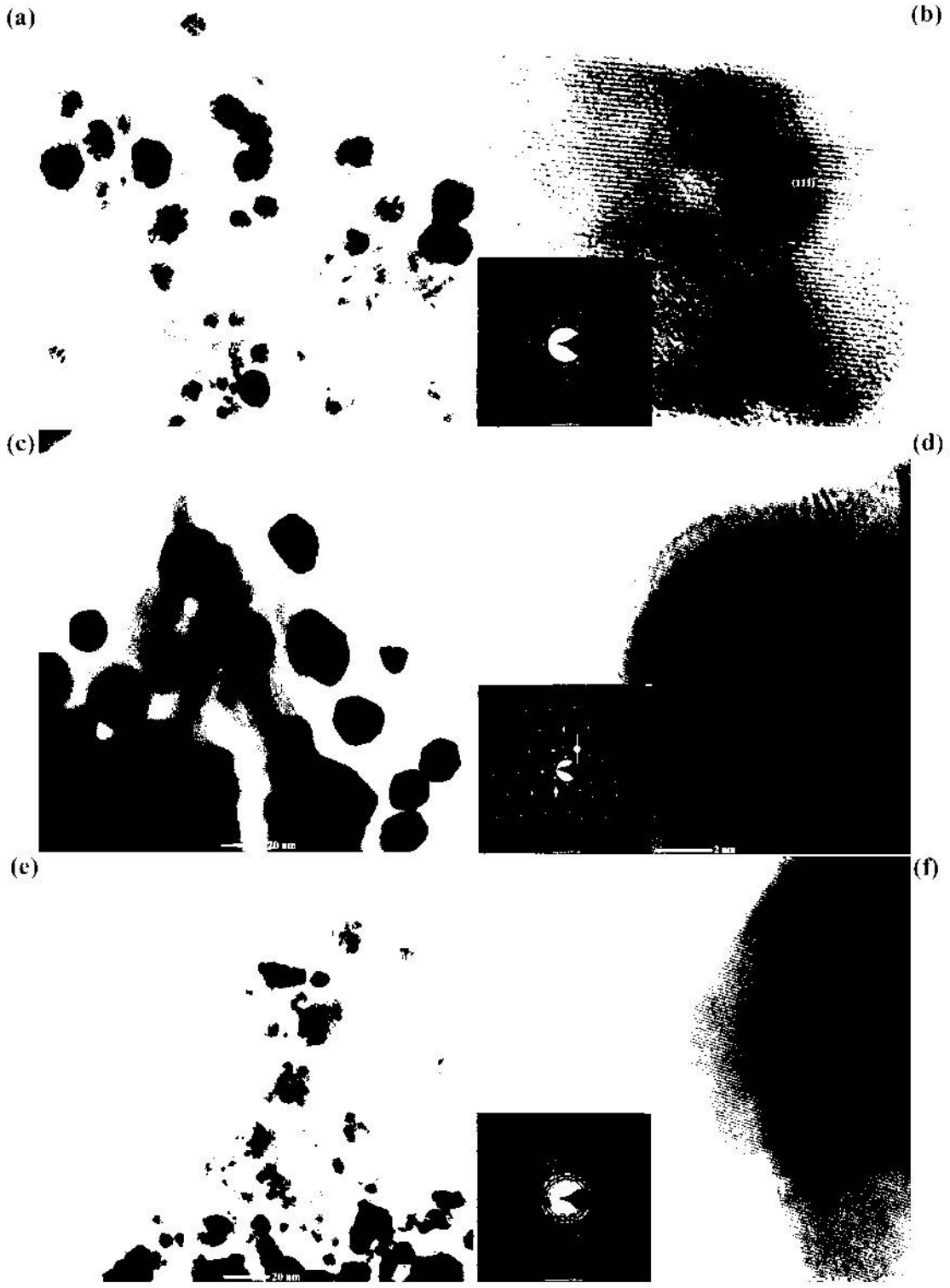

Figure 3. TEM images of (a) and (b) Ag–GO, (c) and (d) Au–GO and (e) and (f) Ag–Au–GO.

presence of C–C (284.5 eV), C–O (286.6 eV) and C=O (288.4 eV). Figure 4(c) shows the XPS spectra of 3d spectral region of Ag in the nanocomposites. It shows two peaks at 368.04 eV and 373.54 eV respectively corresponding to $Ag3d_{5/2}$ and $Ag3d_{3/2}$ [10]. These peaks were again deconvoluted into two strong peaks at 367.68 and 373.69 eV corresponding to Ag (I) state and, two weak peaks at 368.53 and 373.17 eV corresponding to the Ag (0) state. The appearance of this Ag (I) state indicates the presence of Ag–O species which is in agreement with the results reported by Joshi *et al* [10]. Figure 4(d) shows the XPS spectra of 4f spectral region of Au in the nanocomposites. It showed two main peaks at 83.98 eV and 87.99 eV respectively corresponding to $Au4f_{7/2}$ and $Au4f_{5/2}$ [16]. These peaks again de-convoluted into two strong peaks at 83.87 and 87.91 eV

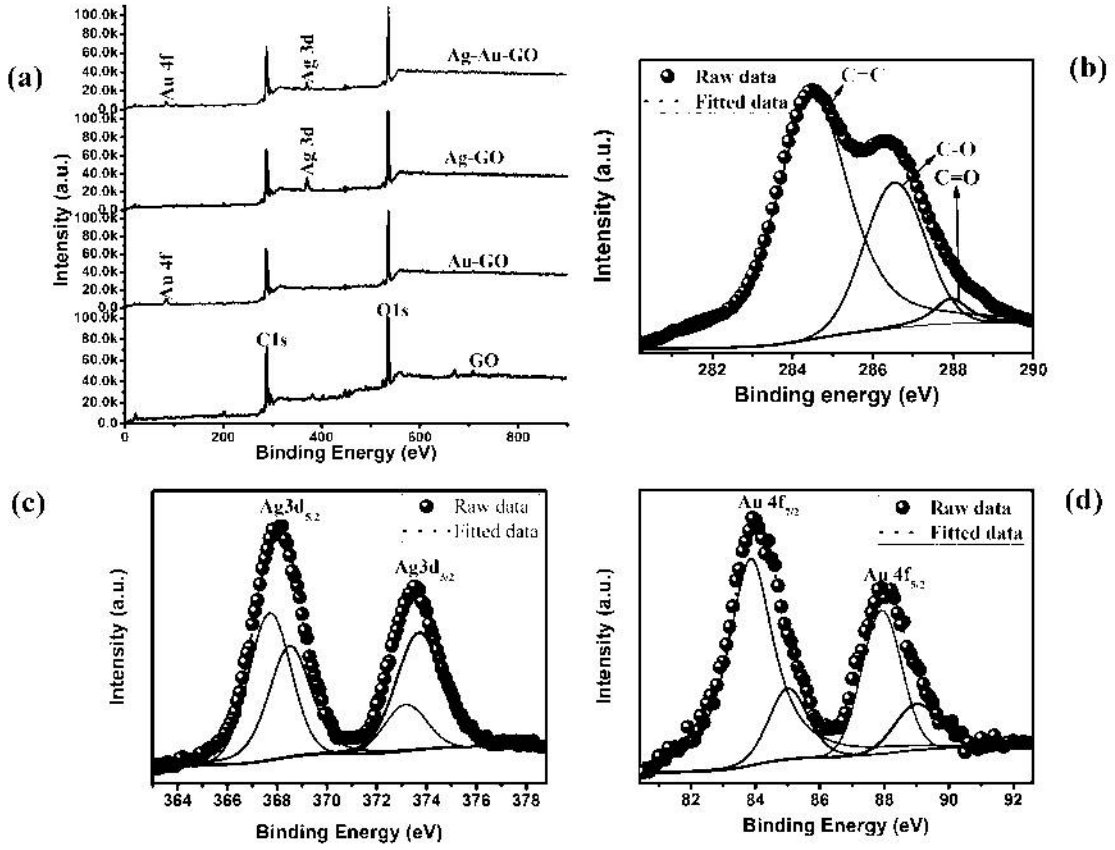

Figure 4. (a) XPS survey spectra of GO, Ag–GO, Au–GO and Ag–Au–GO nanocomposites, high resolution XPS spectra of (b) C1s of GO's, (c) Ag 3d and (d) Au 4f.

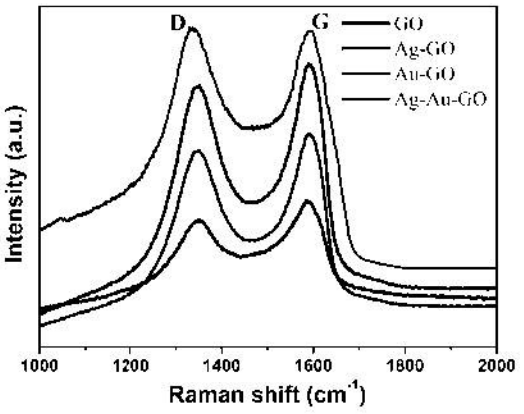

Figure 5. Raman spectroscopy of GO, Ag–GO, Au–GO and Ag–Au–GO nanocomposites.

corresponding to Au (0) state and, two weak peaks at 85.04 and 89.03 eV corresponding to Au^{+} state [17]. These small peaks correspond to the formation of gold oxide species [16].

Raman spectroscopy for Ag–GO, Au–GO and Ag–Au–GO nanocomposites along with GO is as shown in figure 5. GO exhibits its characteristic D band and G band around 1350 and 1588 cm^{-1} respectively [18]. The intensity ratio of D to G band (I_D/I_G) is found to be 0.89 for GO. The synthesized nanocomposites also showed similar kind of peaks but the intensity ratio of D to G band (I_D/I_G) is increased to 0.92, 0.93 and 1.01 respectively for Ag–GO, Au–GO and Ag–Au–GO nanocomposites. This increase in the I_D/I_G indicates the decoration of nanoparticles on GO sheets [10].

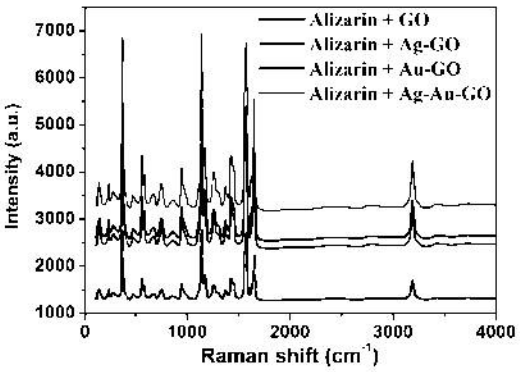

Figure 6. SERS for GO, Ag–GO, Au–GO and Ag–Au–GO samples.

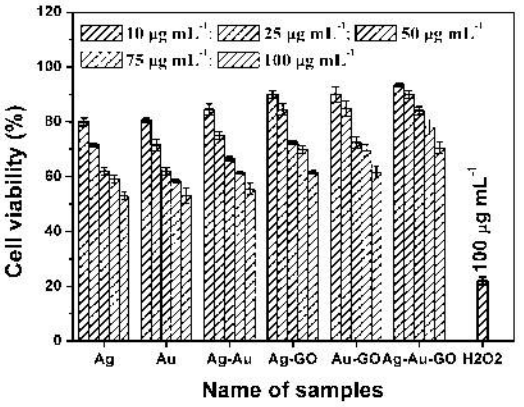

Figure 7. Cell viability of Chang liver cell lines for 24 h using MTT assay for Ag, Au, Ag–Au, Ag–GO, Au–GO and Ag–Au–GO samples.

3.2. Surface enhanced Raman spectroscopy of nanocomposites

SERS of the prepared nanocomposites Ag–GO, Au–GO and Ag–Au–GO with alizarin has been studied. Figure 6 shows the SERS for GO, Ag–GO, Au–GO and Ag–Au–GO with alizarin excited at a wavelength of 634 nm, while that of Ag, Au, Ag–Au is shown in figure S3 (ESI). The reproducibility of the SERS measurements was achieved by recording the spectra from different spots on the same substrate with the relative standard deviation was around 10%. The peaks at 138, 225, 367, 562, 747, 932, 1149, 1258, 1431, 1562, 1660 and 3192 cm^{-1} are due to alizarin [19]. It can be seen from figure 6 that the SERS intensity of nanocomposites is more than that of respective bare nanoparticles of the same concentrations. This enhanced SERS intensity of the nanocomposite materials may be due to the electromagnetic enhancement which arises due to the large local fields as a result of surface plasmon resonance [30, 31]. It can also be observed that Ag–Au–GO nanocomposite exhibits more SERS intensity compared to that of Ag–GO and Au–GO nanocomposite. This may be due to the combined surface plasmon resonance of Ag and Au which results in more electromagnetic enhancement compared to individual ones.

3.3. Cell viability of nanocomposites

An MTT assay was used to study the effect of Ag, Au, Ag–Au, Ag–GO, Au–GO and Ag–Au–GO nanocomposites on the cell viability of Chang liver cell lines. The respective results are shown in figure 7 for nanocomposites along with bare nanoparticles for 24 h and that for 48 h is shown in figure S4 (ESI). It can be seen from figure 7 that the percentage of cell viability, which decreases with increase in concentration of both bare nanoparticles and nanocomposites, may be due to the increase in concentration of Ag and Au. It is also interesting to observe that the nanocomposites showed enhanced cell viability above that of bare nanoparticles which can be explained as follows. The bare nanoparticles may agglomerate with each other and results in less phytochemicals (from Neem leaves extract) carried by them. However, in the case of nanocomposites, the agglomeration of nanoparticles will be controlled by GO sheet [10] and will result in more phytochemicals carried by them [37]. These phytochemicals may protect stress-induced apoptotic DNA fragmentation or DNA lesion [32] which

results in enhancement in cell viability. This result indicates that the nanocomposites show less toxicity effects and may protect DNA lesion in cultured Chang liver cells.

4. Conclusions

The bio-green one-pot method has been adopted for the synthesis of Ag–GO, Au–GO and Ag–Au–GO nanocomposites using *Azadirachta indica*. UV–visible spectroscopy, XRD, TEM, Raman spectroscopy and XPS results revealed the decoration of face centered cubic structured nanoparticles of size ~10 nm for Ag, ~20 nm for Au and ~15 nm for Ag–Au on a GO sheet. The synthesized bio-green nanocomposites using *Azadirachta indica* showed enhancement in SERS activity and cell viability compared to bare nanoparticles due to the synergetic interaction between nanoparticles and GO sheet.

Acknowledgments

The author KH would like to thank University Grant Commission, Govt. of India for awarding Dr D S Kothari Post Doctoral Fellowship. The authors thank Jyotsana Dixit for her assistance in preparing Neem leaves extract.

References

[1] Zhu Y, Murali S, Cai W, Li X, Suk J W, Potts J R and Ruoff R S 2010 Graphene and graphene oxide: synthesis, properties, and applications *Adv. Mater.* 22 3906–24
[2] Chen D, Feng H and Li J 2012 Graphene oxide: preparation, functionalization, and electrochemical applications *Chem. Rev.* 112 6027–53
[3] Muszynski R, Seger B and Kamat P V 2008 Decorating graphene sheets with gold nanoparticles *J. Phys. Chem.* C 112 5263–6
[4] Pasricha R, Gupta S and Srivastava A K 2009 A facile and novel synthesis of Ag–graphene-based nanocomposite *Small* 5 2253–9
[5] Li B, Zhnag X, Chen P, Li X, Wang L, Zhang C, Zheng W and Liu Y 2014 Waveband-dependent photochemical processing of graphene oxide in fabricating reduced graphene oxide film and graphene oxide–Ag nanoparticles film *RSC Adv.* 4 2404–8
[6] Khurana G, Misra P, Kumar N, Kooriyattil S, Scott J F and Katiyar R S 2016 Enhanced resistive switching in forming-free graphene oxide films embedded with gold nanoparticles deposited by electrophoresis *Nanotechnology* 27 015702
[7] Wu T, Gao J, Xu X, Wang W, Gao C and Qiu H 2013 A new rapid chemical route to prepare reduced graphene oxide using copper metal nanoparticles *Nanotechnology* 24 215604
[8] Ji Z, Shen X, Li M, Zhou H, Zhu G and Chen K 2013 Synthesis of reduced graphene oxide/CeO_2 nanocomposites and their photocatalytic properties *Nanotechnology* 24 115603
[9] Wu T, Zhang L, Gao J, Liu Y, Gao C and Yan J 2013 Fabrication of graphene oxide decorated with Au–Ag alloy nanoparticles and its superior catalytic performance for the reduction of 4-nitrophenol *J. Mater. Chem.* A 1 7384–90
[10] Joshi A C, Markad G B and Haram S K 2015 Rudimentary simple method for the decoration of graphene oxide with silver nanoparticles: their application for the amperometric detection of glucose in the human blood samples *Electrochim. Acta* 161 108–14
[11] Song J, Xu L, Xing R, Li Q, Zhou C, Liu D and Song H 2014 Synthesis of Au/graphene oxide composites for selective and sensitive electrochemical detection of ascorbic acid *Sci. Rep.* 4 7515
[12] Hsu K C and Chen D H 2014 Green synthesis and synergistic catalytic effect of Ag/reduced graphene oxide nanocomposite *Nanoscale Res. Lett.* 4 484
[13] Neppolian B, Wang C and Ashokkumar M 2014 Sonochemically synthesized mono and bimetallic Au–Ag reduced graphene oxide based nanocomposites with enhanced catalytic activity *Ultrason. Sonochem.* 21 1948–53
[14] Cheng C E, Tsai C W, Pei Z, Lin T W, Chang C S and Chien F S S 2015 UV-treated graphene oxide as anode interfacial layers for P3HT: PCBM solar cells *J. Phys. D: Appl. Phys.* 48 255103
[15] Ajayi O A, Guitierrez D H, Peaslee D, Cheng A, Gao T, Wong C W and Chen B 2015 Electrophoretically deposited graphene oxide and carbon nanotube composite for electrochemical capacitors *Nanotechnology* 26 415203
[16] Yang B, Liu Z, Guo Z, Zhang W, Wan M, Qin X and Zhong H 2014 *In situ* green synthesis of silver–graphene oxide nanocomposites by using tryptophan as a reducing and stabilizing agent and their application in SERS *Appl. Surf. Sci.* 316 222–7
[17] Gupta V K, Atar N, Yola M L, Eryilmaz M, Torul H, Tamer U, Boyaci I H and Ustundag Z 2013 A novel glucose biosensor platform based on Ag@AuNPs modified graphene oxide nanocomposite and SERS application *J. Colloid Interface Sci.* 406 231–7
[18] Wang N, Hu B, Chen M L and Wang J H 2015 Polyethylenimine mediated silver nanoparticle-decorated magnetic graphene as a promising photothermal antibacterial agent *Nanotechnology* 26 195703
[19] Hou L, Feng Q, Wang Y, Yang X, Ren J, Shi Y, Shan X, Yuan Y, Wang Y and Zhnag Z 2016 Multifunctional hyaluronic acid modified graphene oxide loaded with mitoxantrone for overcoming drug resistance in cancer *Nanotechnology* 27 015701
[20] Zhu X, Zhnag H, Huang H, Zhnag Y, Hou L and Zhnag Z 2015 Functionalized graphene oxide-based thermosensitive hydrogel for magnetic hyperthermia therapy on tumors *Nanotechnology* 26 365103
[21] Shen J, Shi M, Yan B, Ma H, Li N and Ye M 2011 One-pot hydrothermal synthesis of Ag-reduced graphene oxide composite with ionic liquid *J. Mater. Chem.* 21 7795–801
[22] Li J, Liu C and Liu Y 2012 Au/graphene hydrogel: synthesis, characterization and its use for catalytic reduction of 4-nitrophenol *J. Mater. Chem.* 22 8426–30
[23] Bao Q, Zhang D and Qi P 2011 Synthesis and characterization of silver nanoparticle and graphene oxide nanosheet composites as a bactericidal agent for water disinfection *J. Colloid Interface Sci.* 360 463–70
[24] Das M R, Sarma R K, Saikia R, Kale V S, Shelke M V and Sengupta P 2011 Synthesis of silver nanoparticles in an aqueous suspension of graphene oxide sheets and its antimicrobial activity *Colloids Surf.* B 83 16–22
[25] Hui K S, Hui K N, Dinh D A, Tsang C H, Cho Y R, Zhou W, Hong X and Chun H H 2014 Green synthesis of dimension-controlled silver nanoparticle-graphene oxide with *in situ* ultrasonication *Acta Mater.* 64 326–32